

**Theoretical Study of the Two-Photon Circular Dichroism of Molecular
Structures Simulating Aromatic Amino Acids Residues in Proteins with
Secondary Structures**

Yuly Vesga,¹ Carlos Diaz,¹ Florencio E. Hernandez^{1,2,*}

*¹Department of Chemistry and, ²The College of Optics and Photonics, CREOL, University of
Central Florida, P. O. Box 162366, Orlando, Florida 32816-2366, USA*

** Corresponding Authors: florencio.hernandez@ucf.edu*

Supporting Information

I. THEORETICAL CALCULATIONS:

Geometry optimization of all His, Phe, and Tyr residues were accomplish using density functional theory (DFT) ^{1, 2} at the B3LYP/6-311G(d) and CAM-B3LYP/6-311G(d) ³⁻⁷ level of theory. Excited-states energies (ν_i), oscillator strengths (f_i) and velocity rotatory strengths (R_i) were calculated for the first 80 electronic excited states computed via time dependent-DFT (TD-DFT) ^{1, 2}, at the same level of theory as for the geometry optimizations. Calculations were achieved in gas phase employing Gaussian 09 ⁸.

OPA spectra were calculated by a Gaussian broadening of the oscillator strength according to ⁹:

$$\varepsilon(\nu) = \sum_{i=1}^n \varepsilon_i(\nu) = \sum_{i=1}^n \left(\frac{f_i}{7.653619415 \times 10^{-9} \Gamma} e^{-\left(\frac{\nu-\nu_i}{\Gamma}\right)^2} \right), \quad (1)$$

while ECD spectra were obtained from the velocity rotatory strength applying the Harada-Nakanishi equations ¹⁰:

$$\Delta\varepsilon(\nu) = \sum_{i=1}^n \Delta\varepsilon_i(\nu) = \sum_{i=1}^n \left(\frac{R_i}{2.296 \times 10^{-39} \sqrt{\pi}} \frac{\nu_i}{\Gamma} e^{-\left(\frac{\nu-\nu_i}{\Gamma}\right)^2} \right), \quad (2)$$

where the i subscript denotes to the particular excited state; ν_i is the transition frequency (cm^{-1}) of the excited state of interest, ν is the incident radiation frequency (in cm^{-1}), Γ is the linewidth in wavenumber ($1000 cm^{-1}$ at HW1/eM), f_i is the oscillator strength (dimensionless) and R_i is the velocity rotatory strength ($erg.esu.cm/Gauss$) for the corresponding transition. The values of $\varepsilon_i(\nu)$ and $\Delta\varepsilon_i(\nu)$ have units of $l.mol^{-1}.cm^{-1}$.

Figure S1. Comparative theoretical-experimental ECD plots of L-Alanine (L-Ala), L-Leucine (L-Leu), and L-Valine (L-Val) down to 150 nm (*The experimental data was imported from reference 11*). L-Ala (B3LYP spectrum blue shifted +30 nm and CAM-B3LYP spectrum blue shifted +40 nm); L-Leu (middle) (B3LYP spectrum blue shifted +8 nm and CAM-B3LYP spectrum blue shifted +28 nm); L-Val (top) (B3LYP spectrum blue shifted +20 nm and CAM-B3LYP spectrum blue shifted +40 nm). Theoretical calculations were performed with B3LYP/6-311G* and CAM-B3LYP/6-311G* over the first 20 excited states.

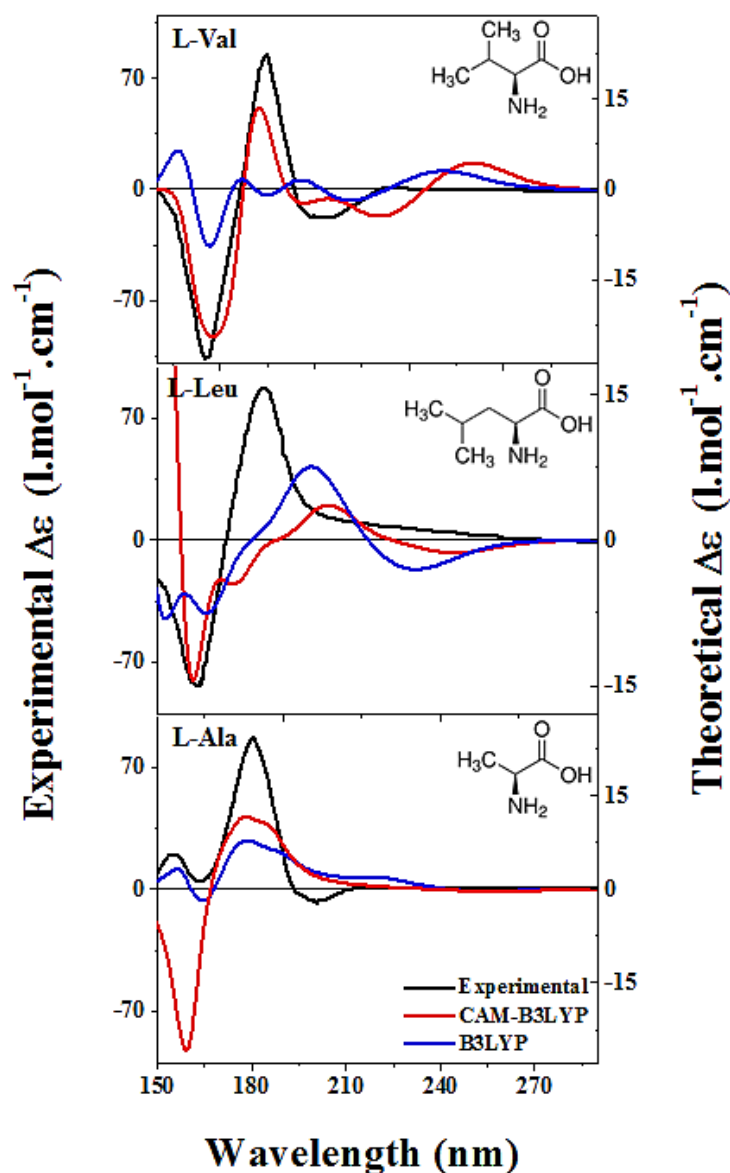
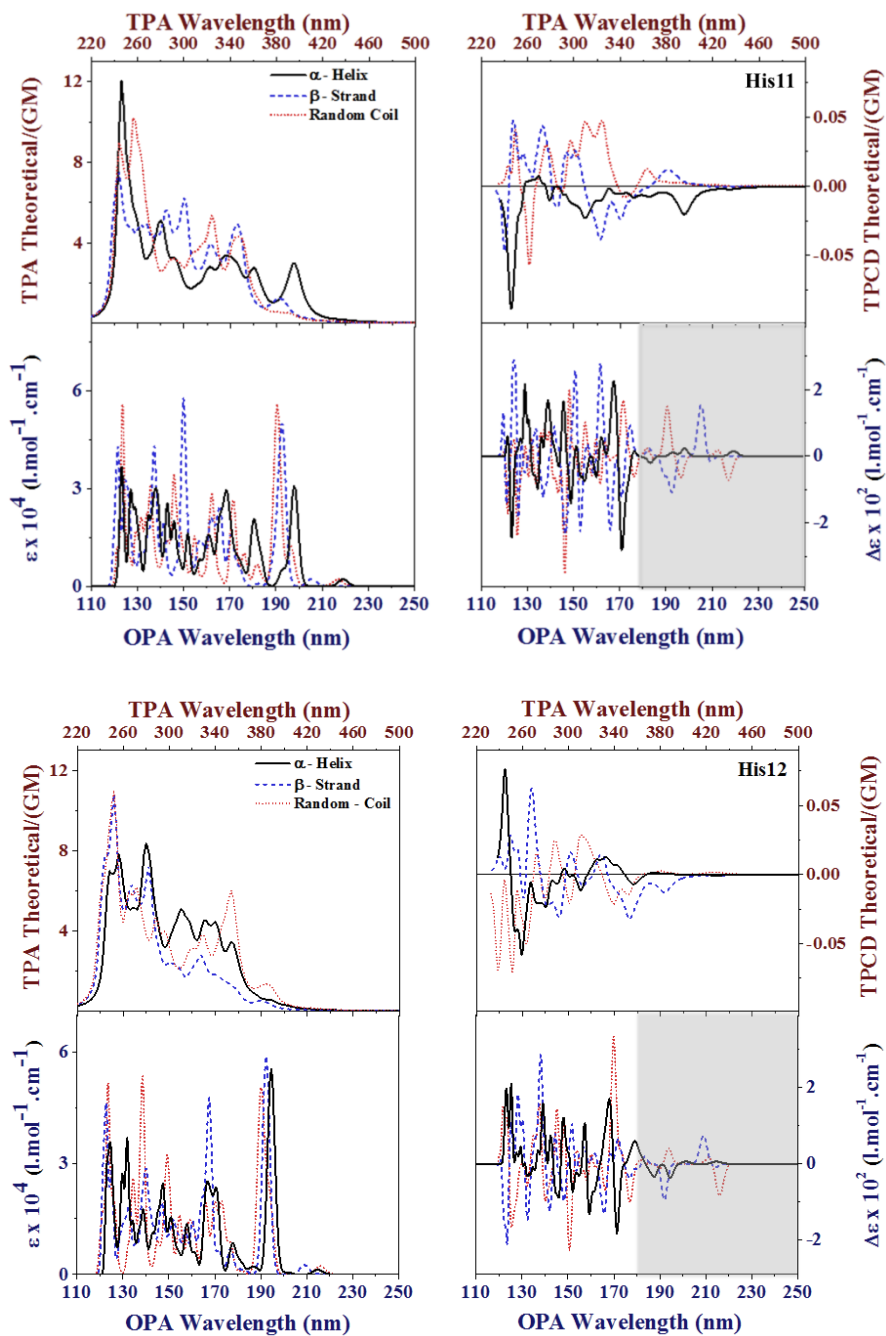
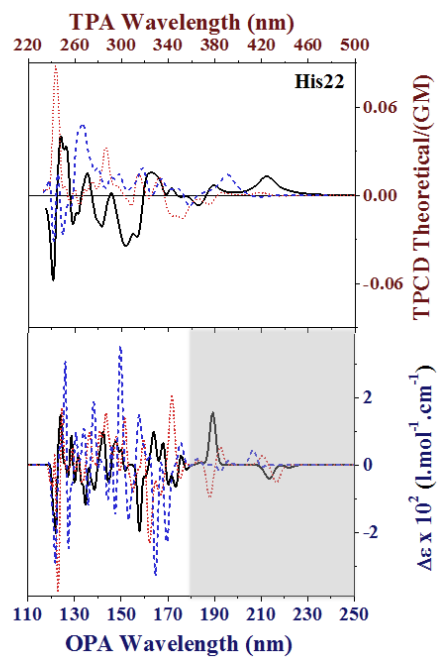
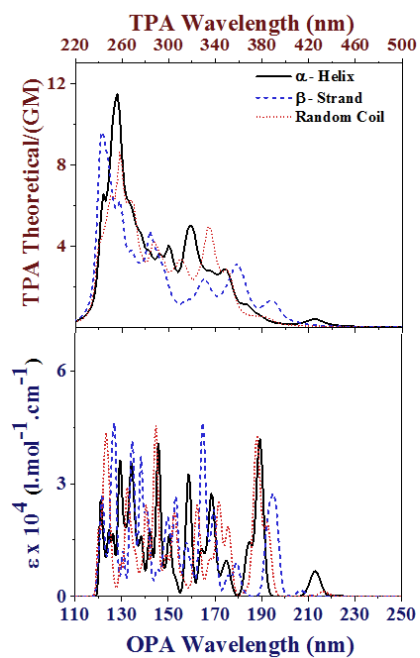
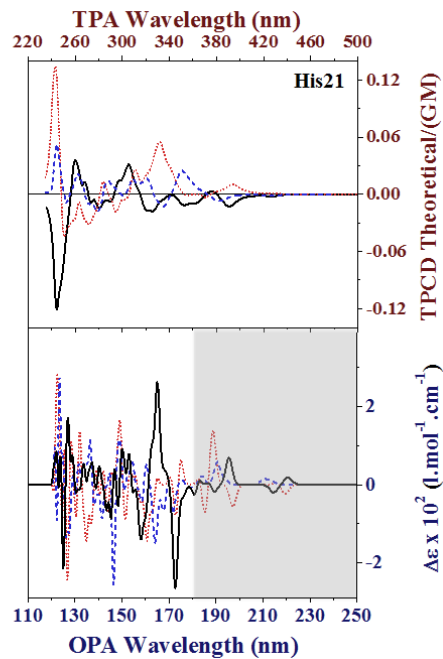
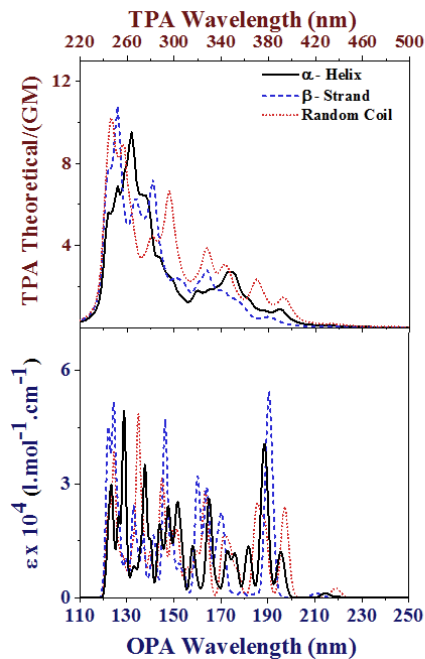


Figure S2. Comparative plots of TPA (top left), TPCD (top right), OPA (bottom left), and ECD (bottom right) spectra of all six His residues in their corresponding random-coil (red dotted line), α -helix (black solid line) and β -strand (blue dashed line) conformations for the lowest 80 electronic excited states of all optimized structures were computed with TD-DFT/ CAM-B3LYP/6-311G(d). Shaded area indicates where ECD is truly functional.





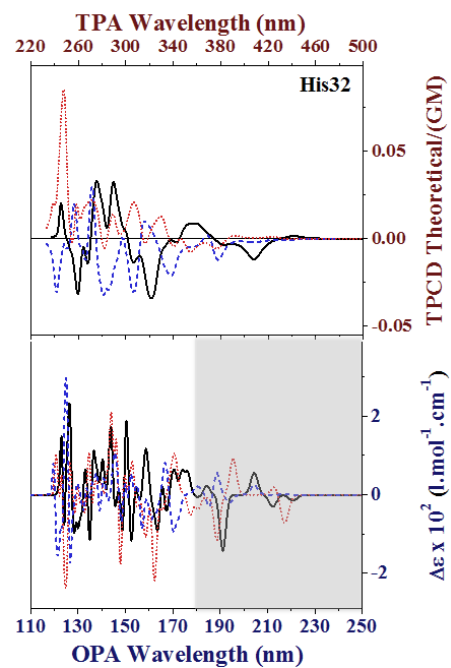
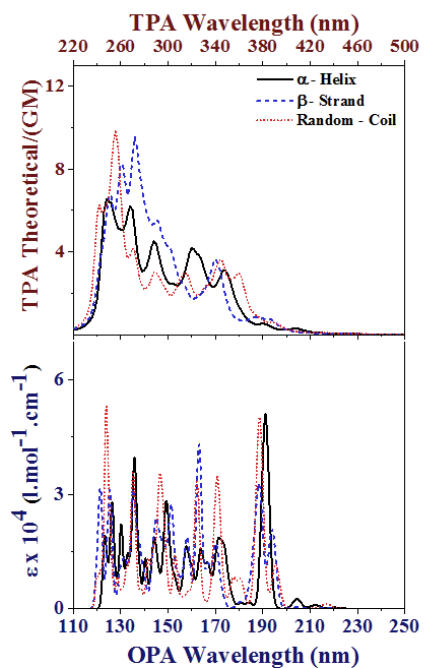
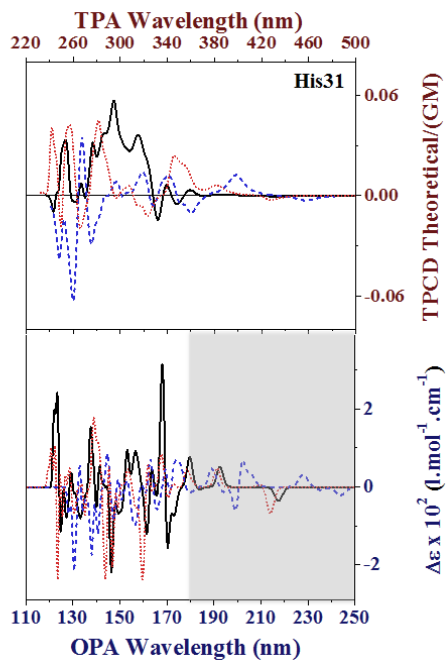
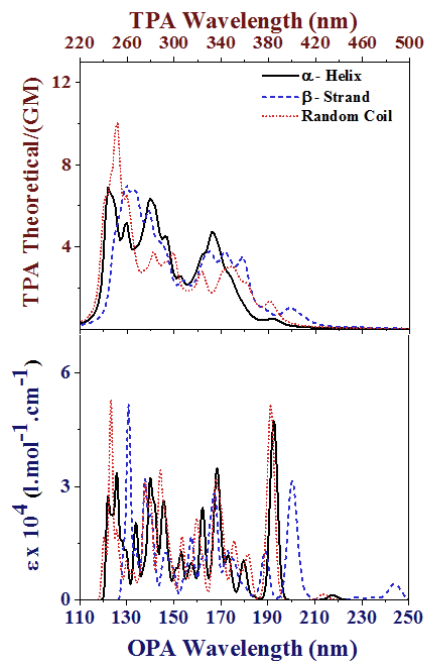
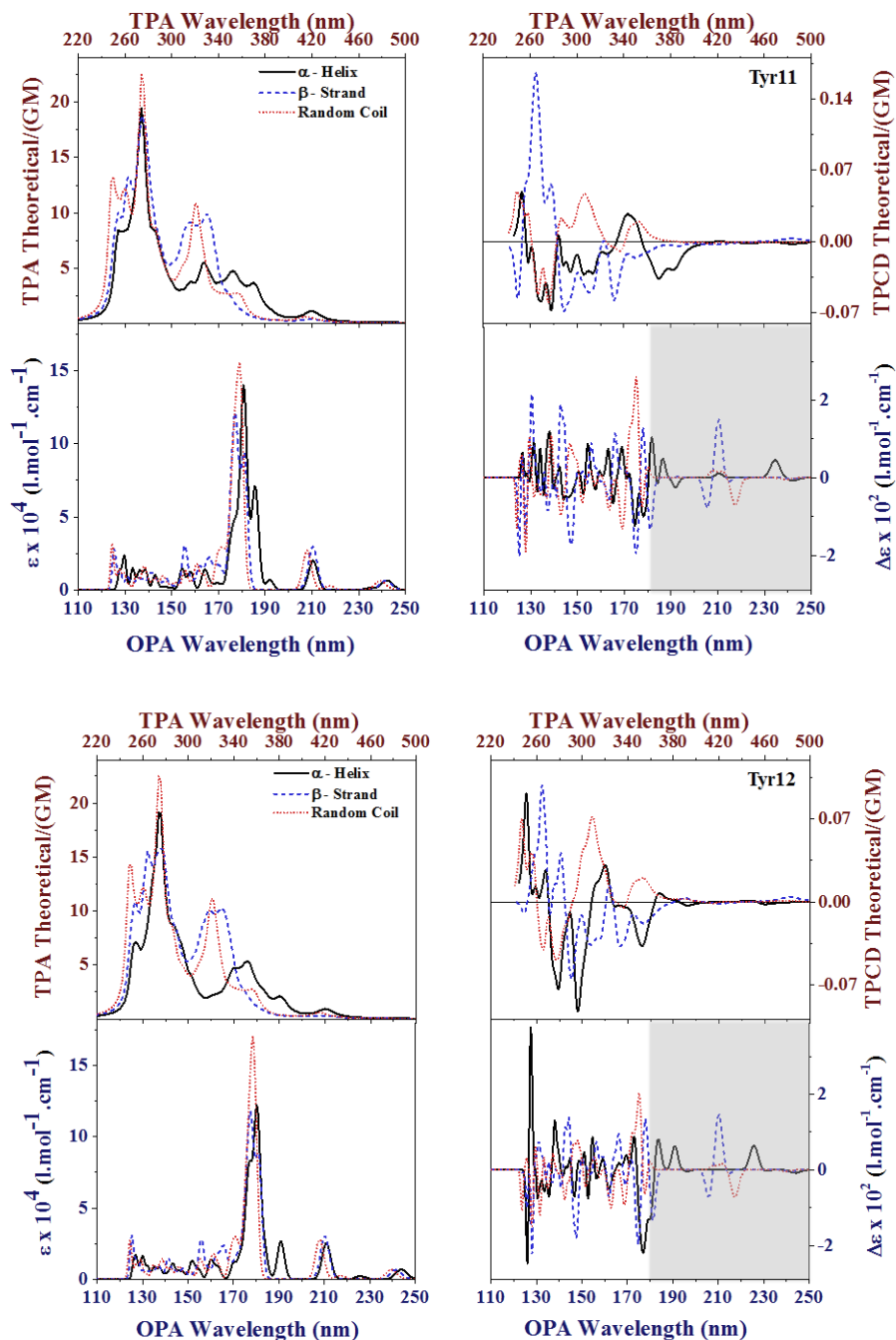
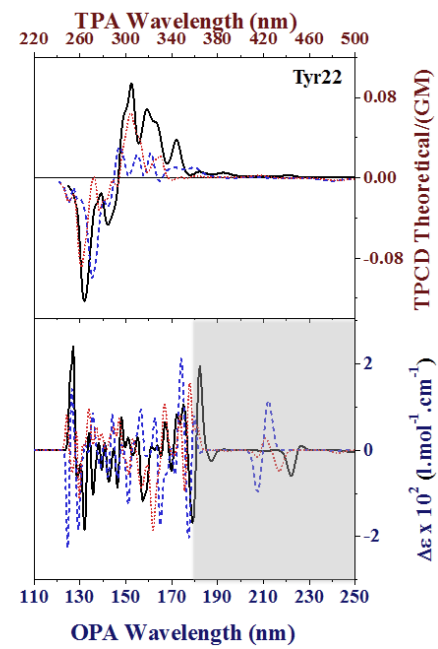
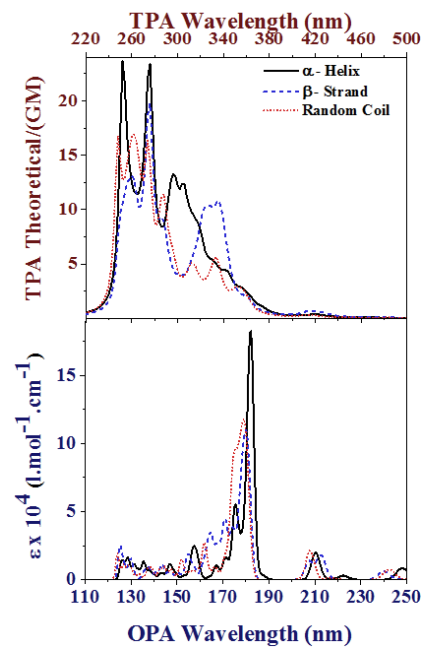
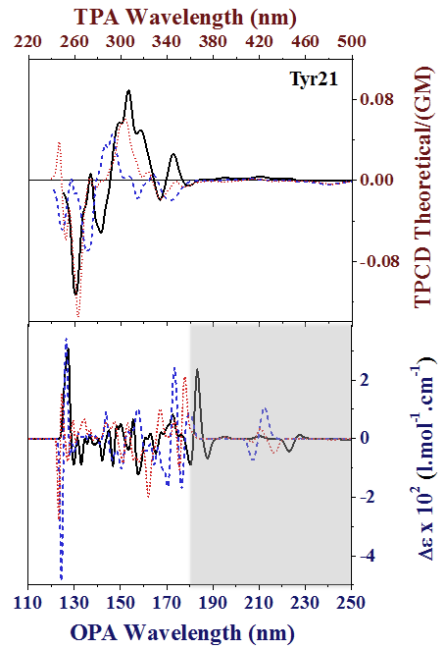
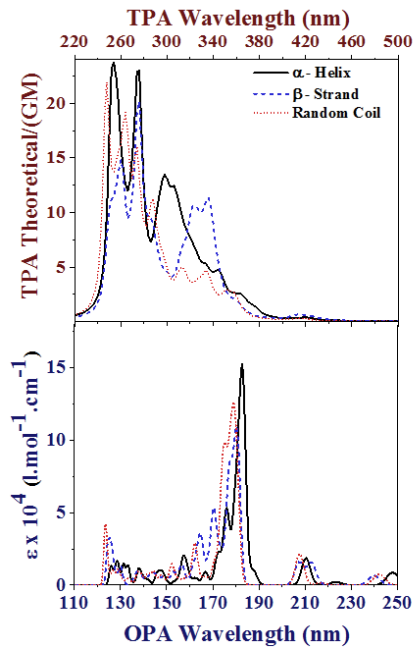


Figure S3. Comparative plots of TPA (top left), TPCD (top right), OPA (bottom left), and ECD (bottom right) spectra of all six Tyr residues in their corresponding random-coil (red dotted line), α -helix (black solid line) and β -strand (blue dashed line) conformations for the lowest 80 electronic excited states of all optimized structures were computed with TD-DFT/ CAM-B3LYP/6-311G(d). Shaded area indicates where ECD is truly functional.





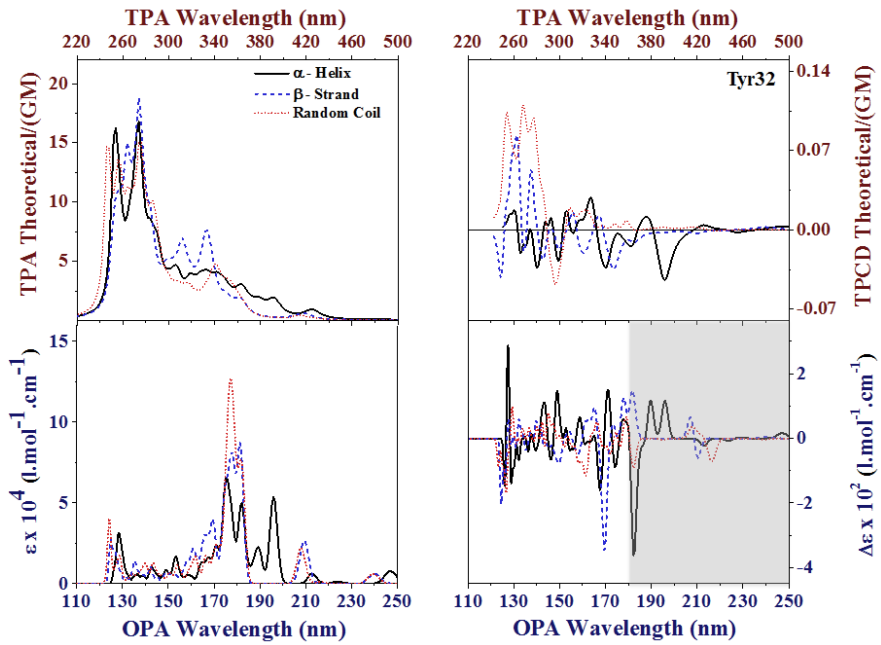
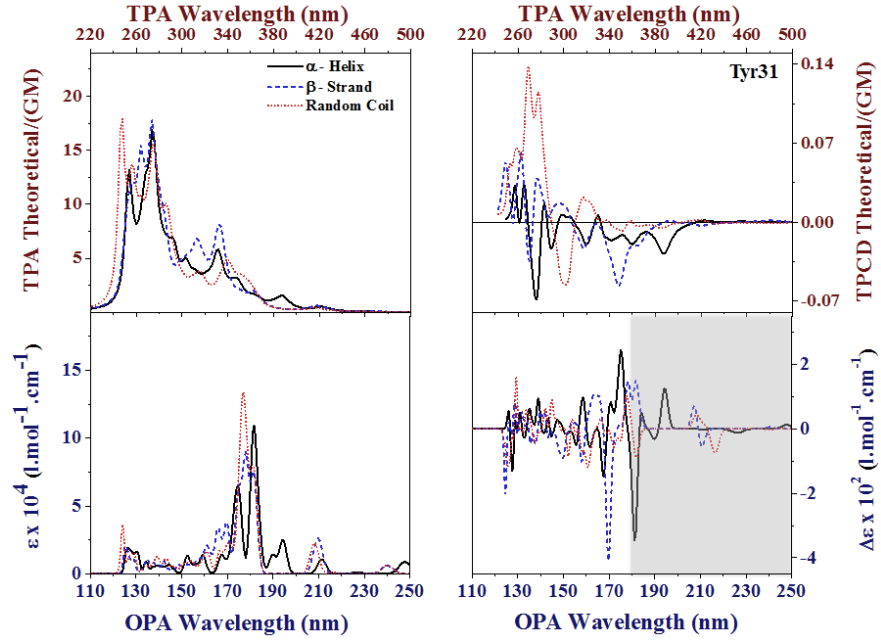
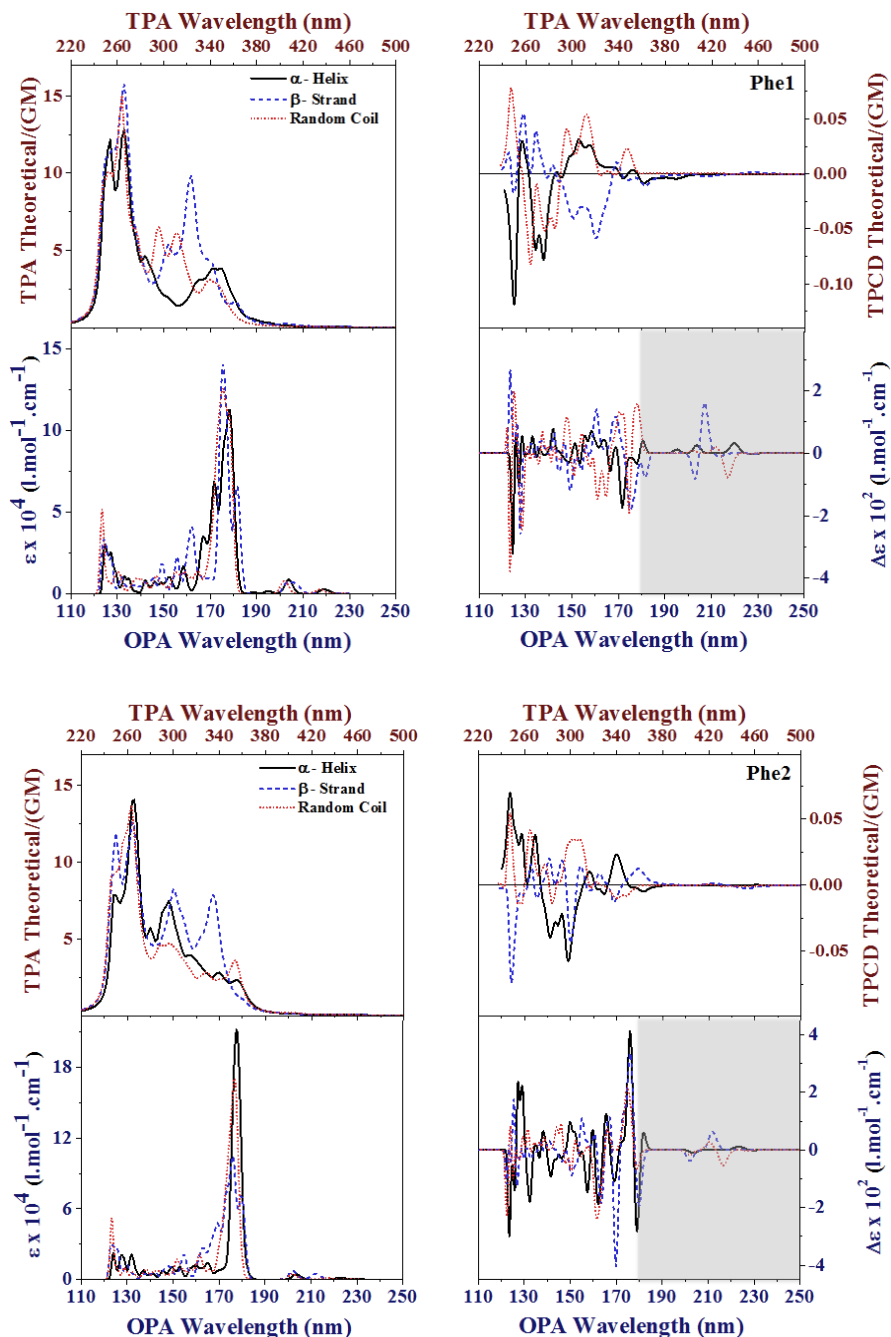


Figure S4. Comparative plots of TPA (top left), TPCD (top right), OPA (bottom left), and ECD (bottom right) spectra of all six Phe residues in their corresponding random-coil (red dotted line), α -helix (black solid line) and β -strand (blue dashed line) conformations for the lowest 80 electronic excited states of all optimized structures were computed with TD-DFT/ CAM-B3LYP/6-311G(d). Shaded area indicates where ECD is truly functional.



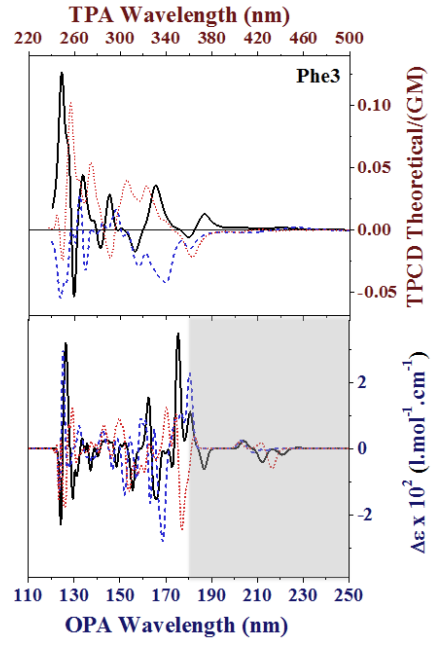
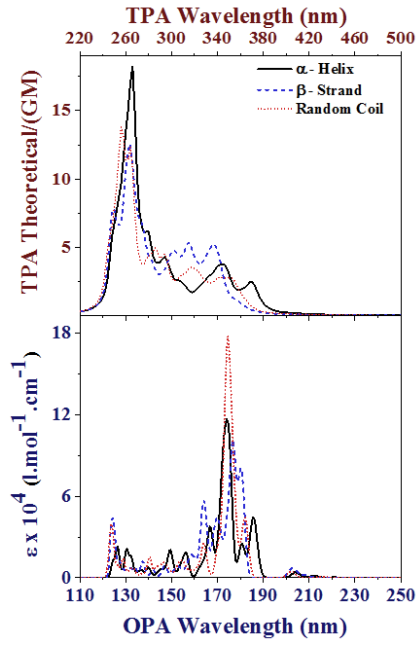
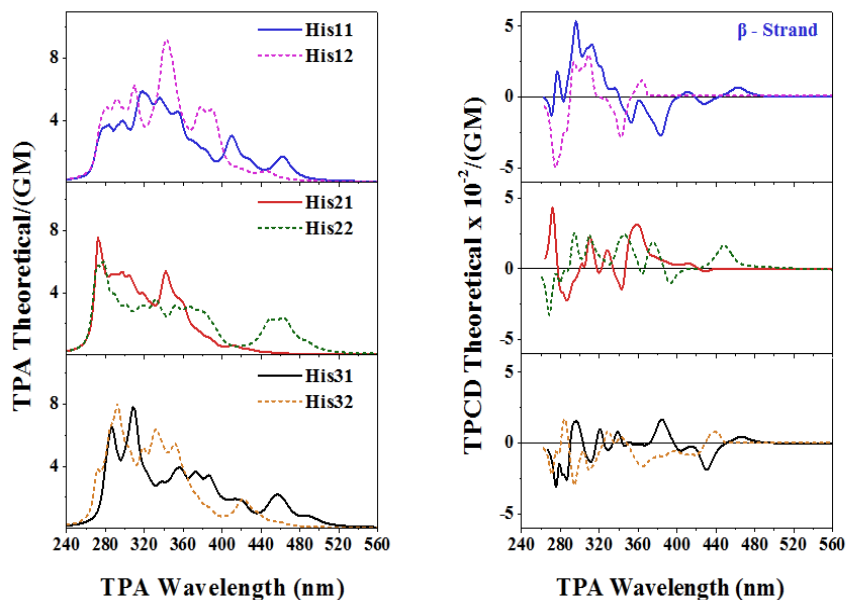
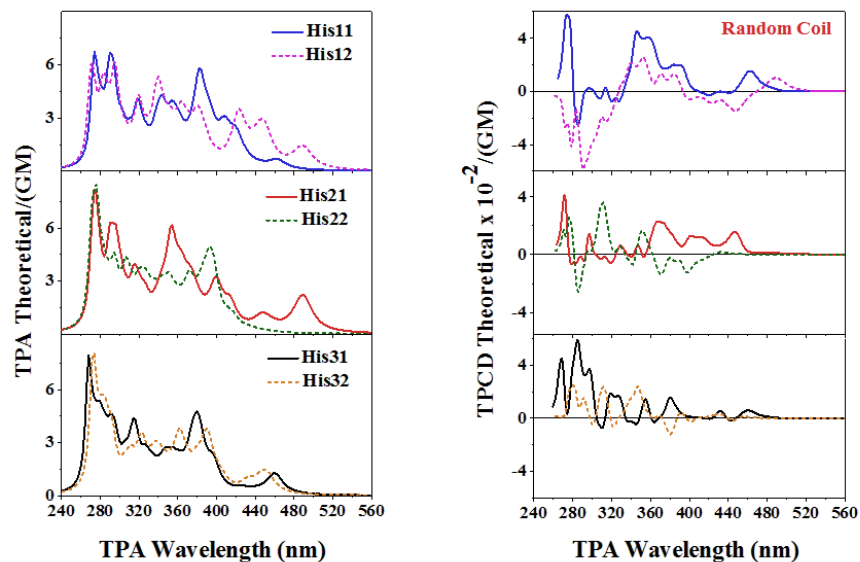


Figure S5. Comparative plots of TPA (left) and TPCD (right) spectra of all six His residues in their corresponding random-coil, β -strand and α -helix conformations. TD-DFT/B3LYP/6-311G(d)/80 excited states.



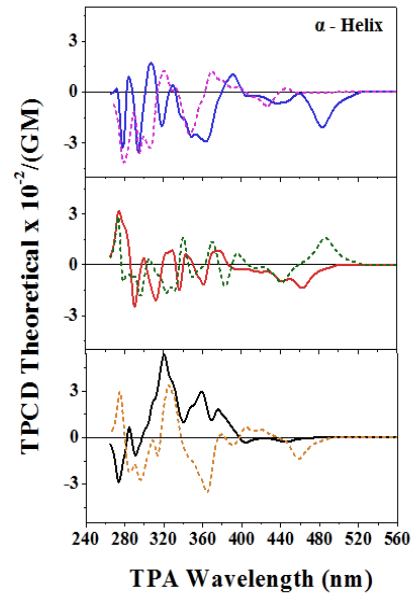
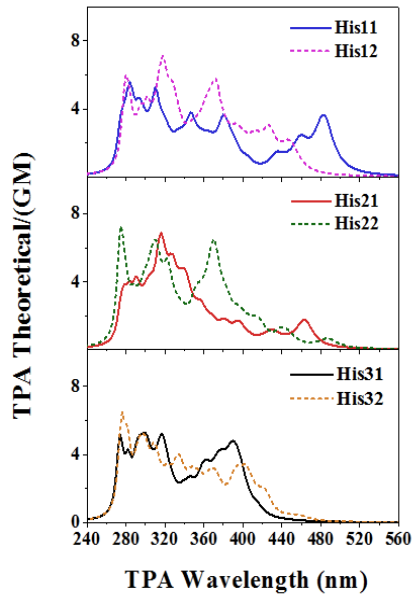
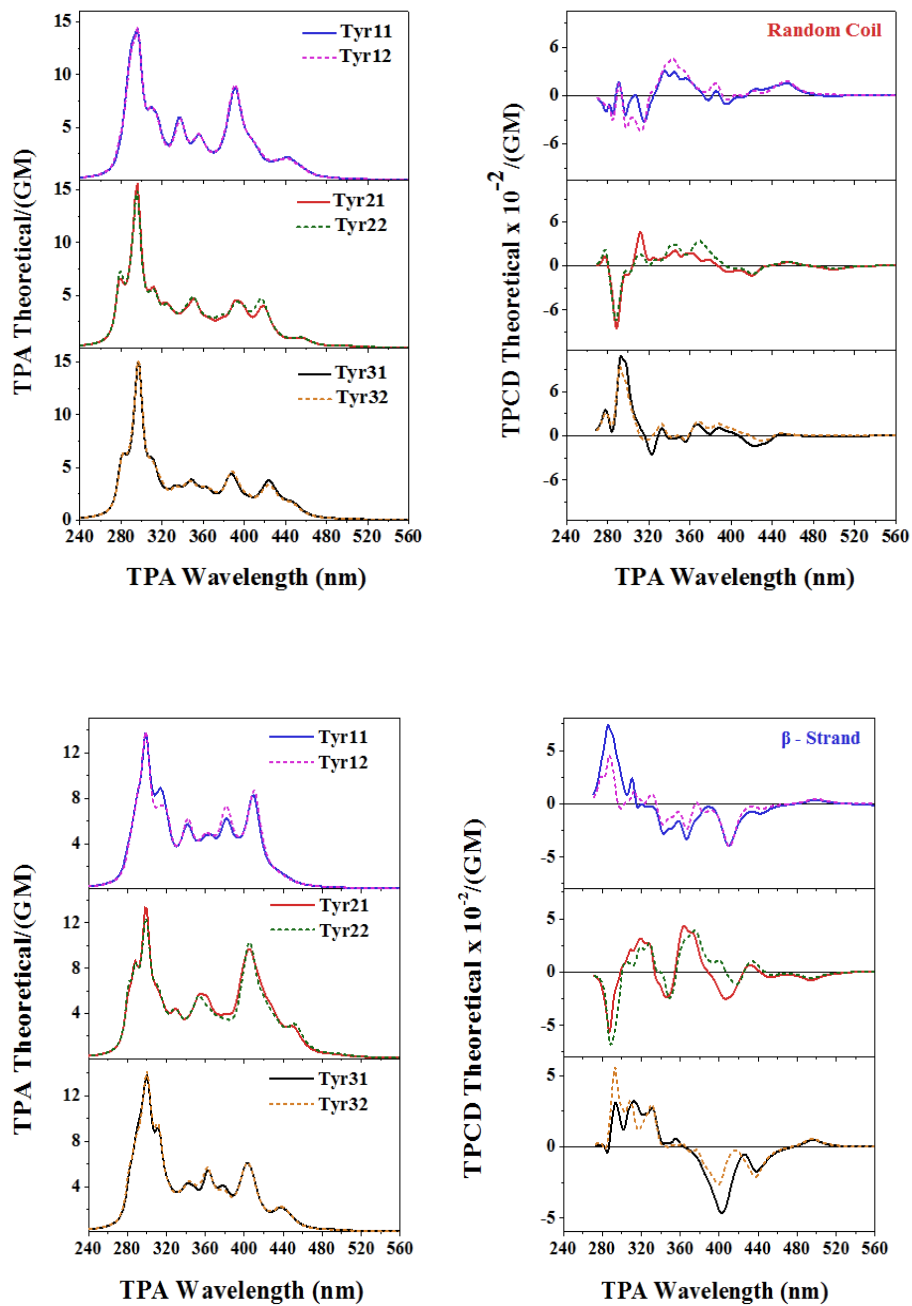


Figure S6. Comparative plots of TPA (left) and TPCD (right) spectra of all six Tyr residues in their corresponding random-coil, β -strand and α -helix conformations. TD-DFT/B3LYP/6-311G(d)/80 excited states.



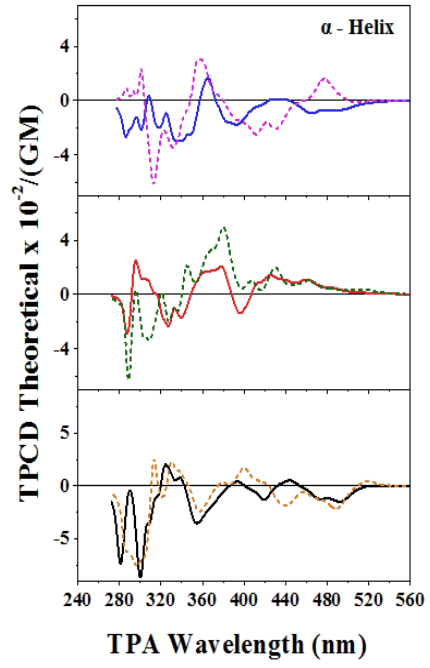
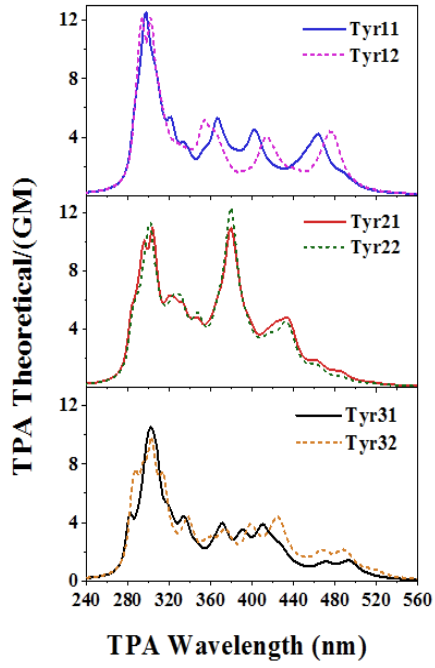


Figure S7. Comparative plots of TPA (left) and TPCD (right) spectra of all three Phe residues in their corresponding random-coil, β -strand and α -helix conformations. TD-DFT/B3LYP/6-311G(d)/80 excited states.

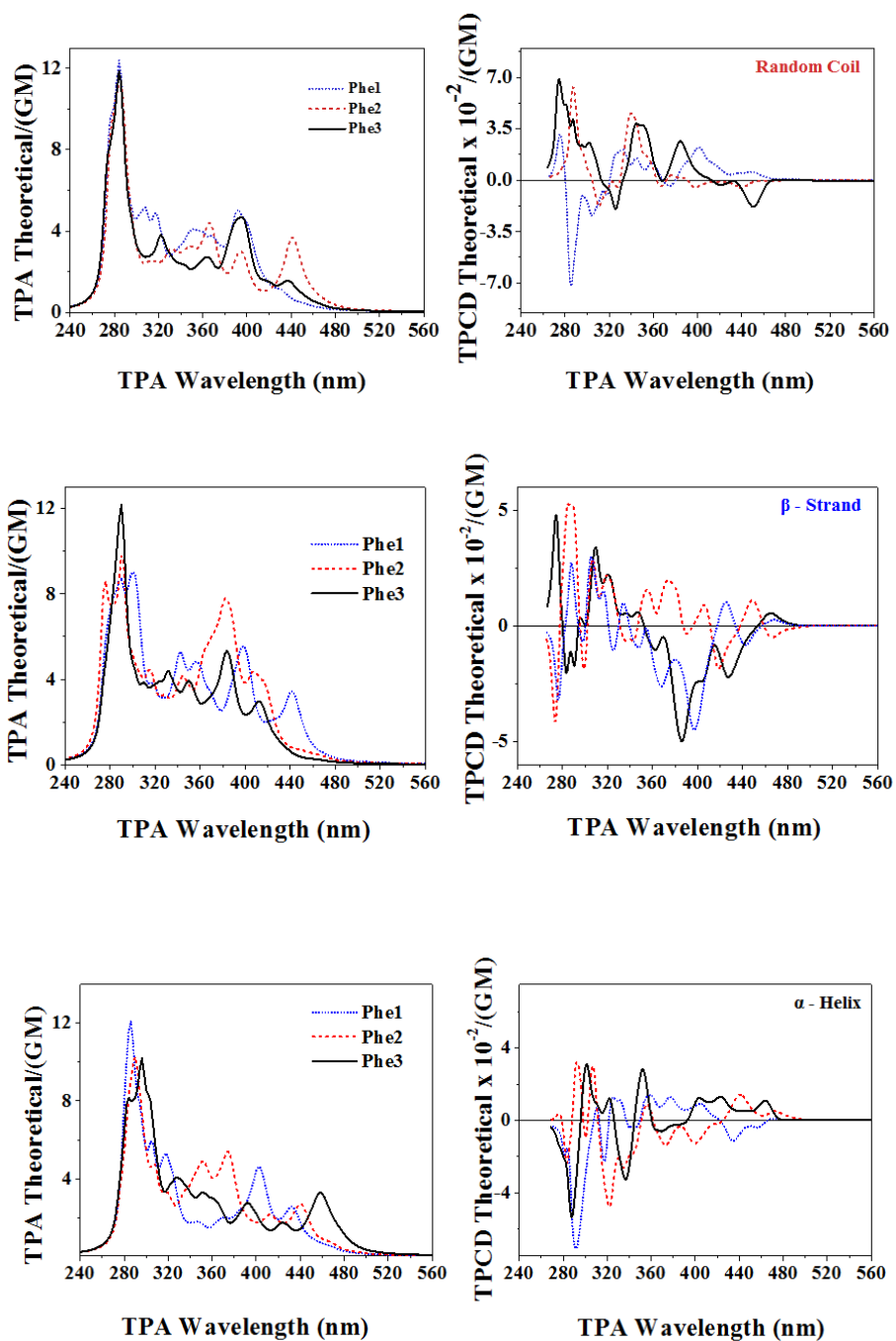
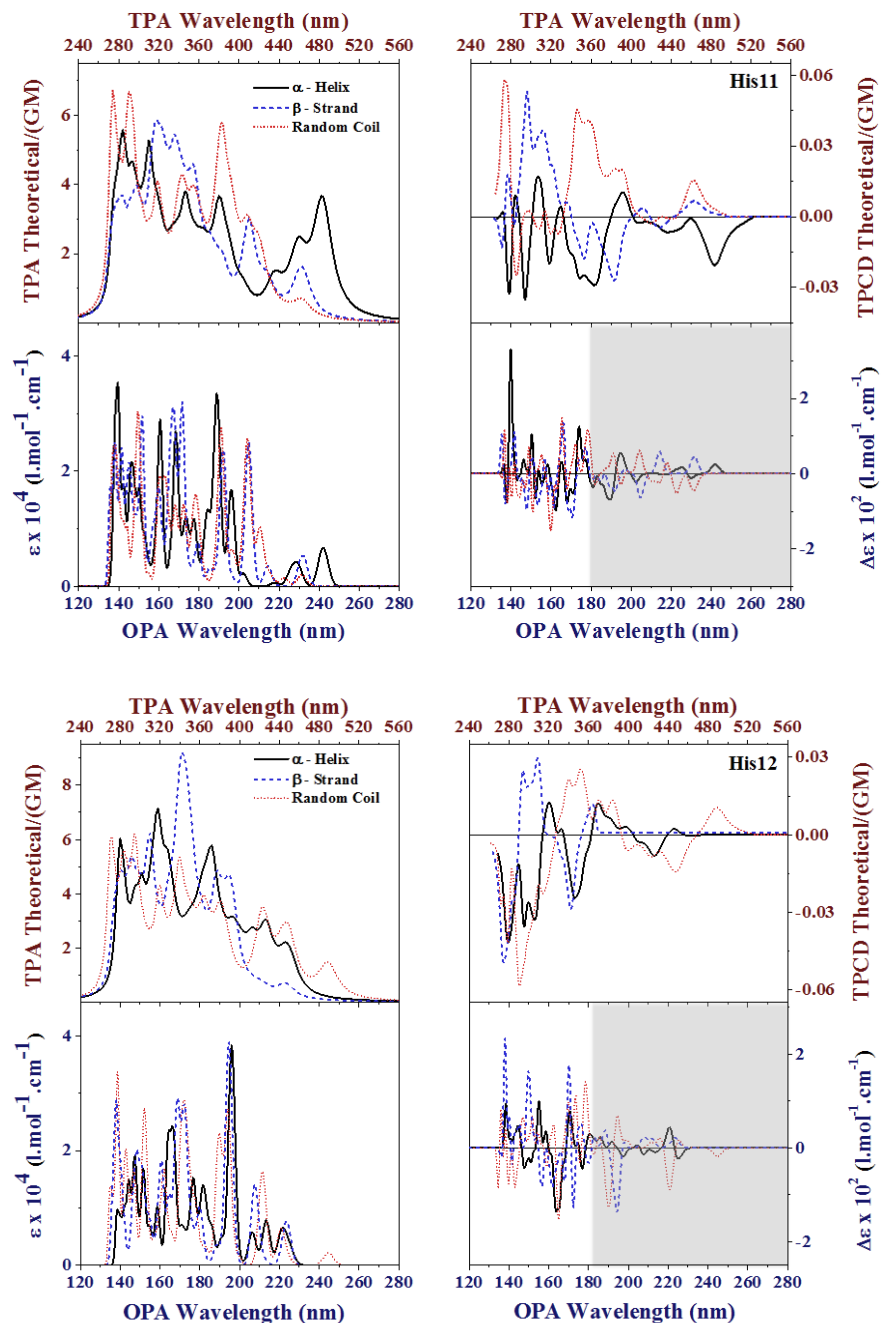
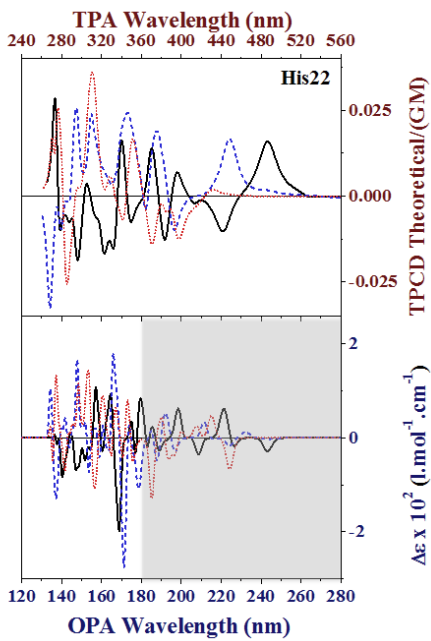
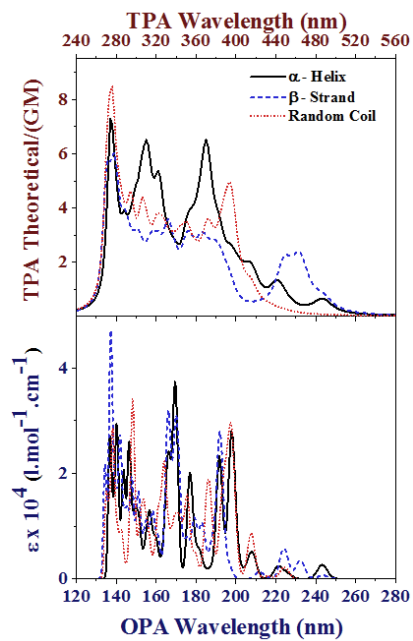
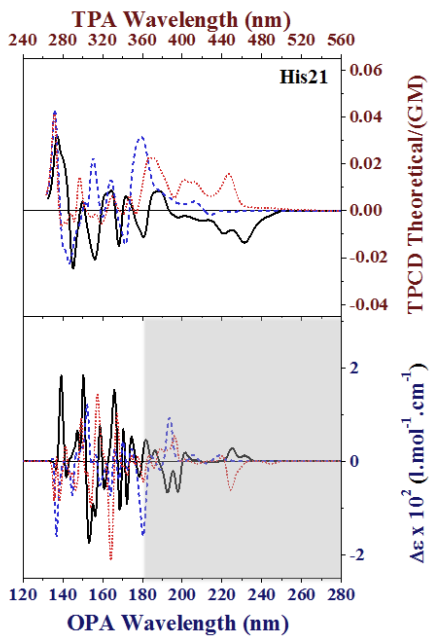
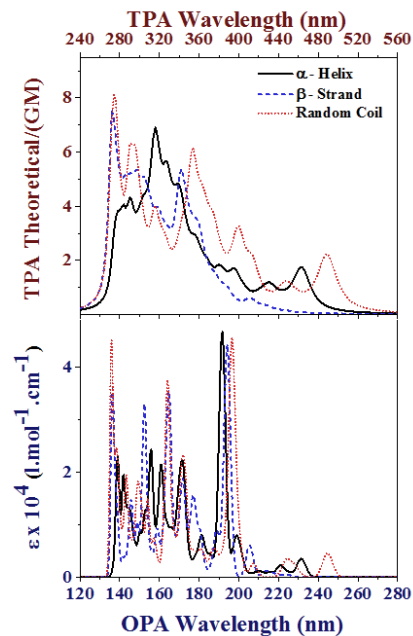


Figure S8. Comparative plots of TPA (top left), TPCD (top right), OPA (bottom left), and ECD (bottom right) spectra of all six His residues in their corresponding random-coil (red dotted line), α -helix (black solid line) and β -strand (blue dashed line) conformations. TD-DFT/ B3LYP/6-311G(d)/80 excited states. Shaded area indicates where ECD is truly functional.





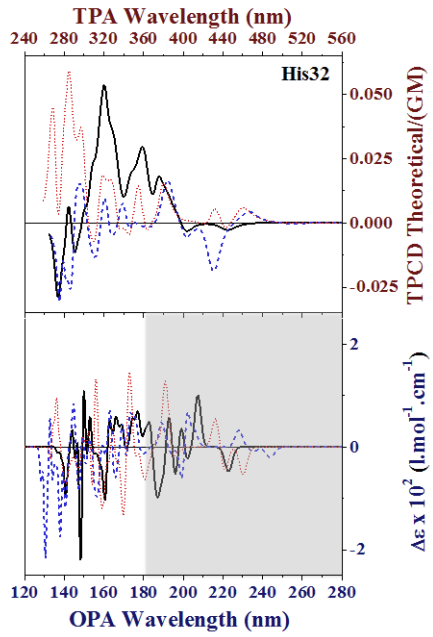
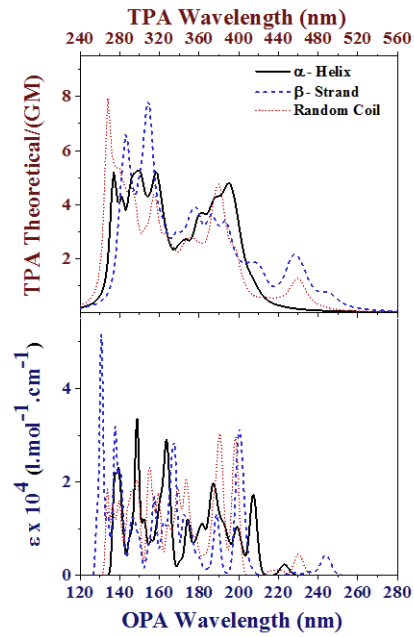
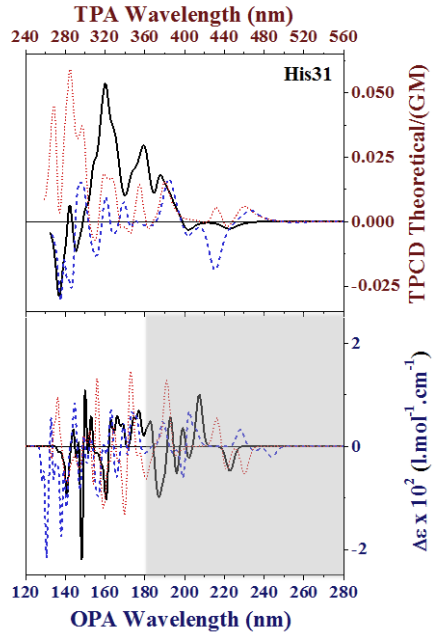
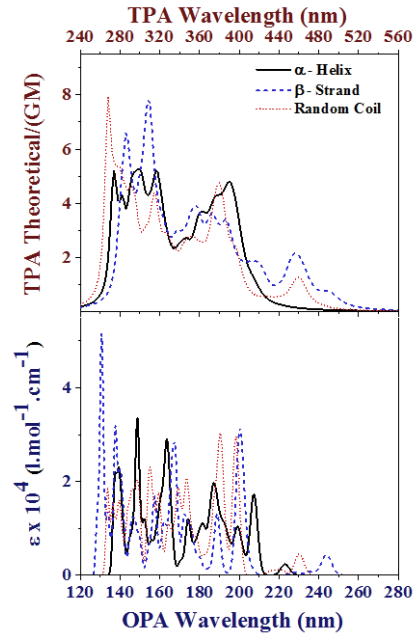
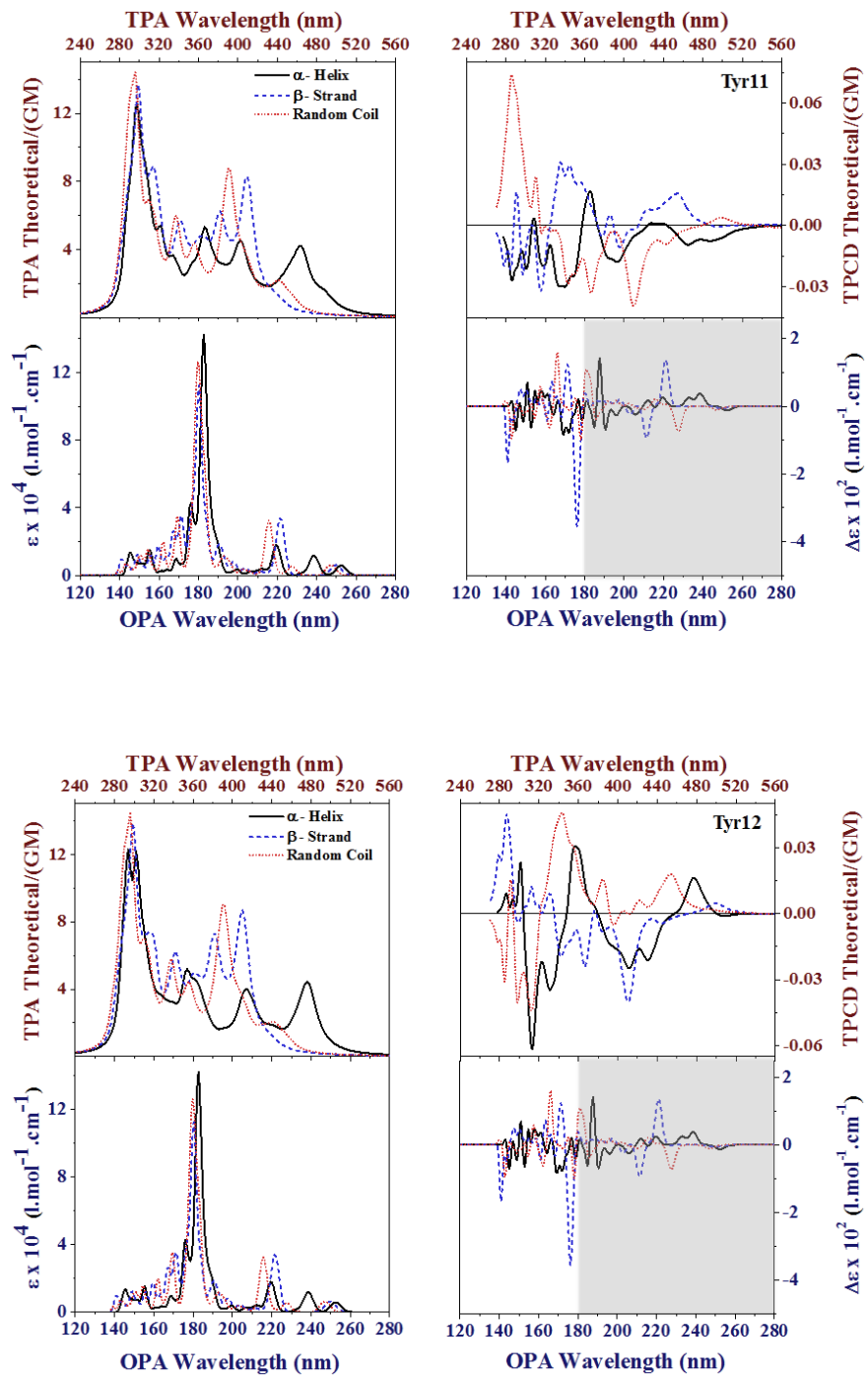
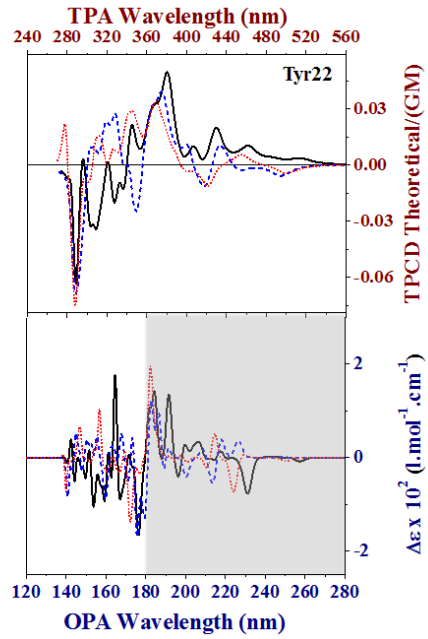
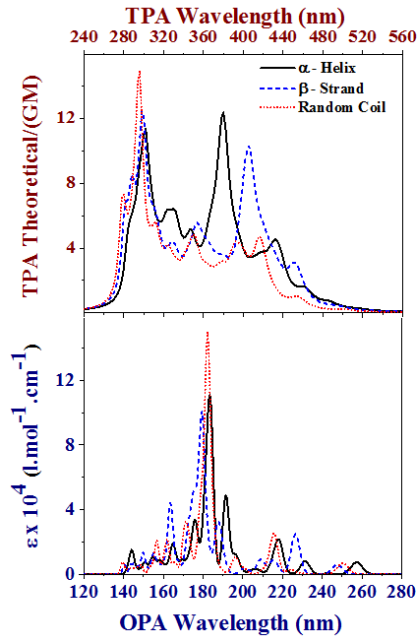
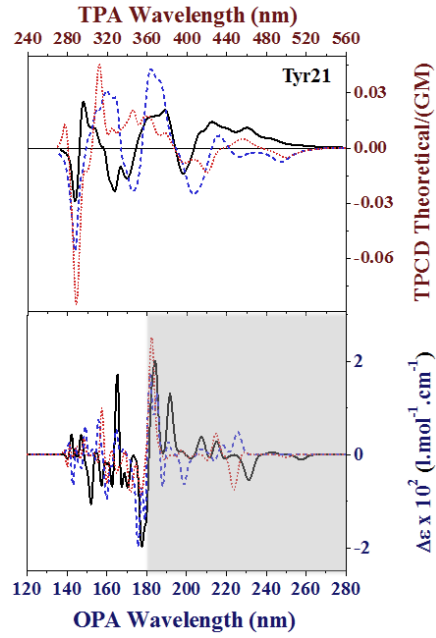
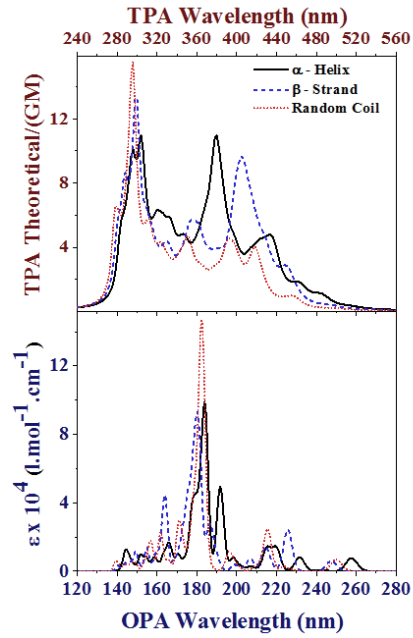


Figure S9. Comparative plots of TPA (top left), TPCD (top right), OPA (bottom left), and ECD (bottom right) spectra of all six Tyr residues in their corresponding random-coil (red dotted line), α -helix (black solid line) and β -strand (blue dashed line) conformations. TD-DFT/ B3LYP/6-311G(d)/80 excited states. Shaded area indicates where ECD is truly functional.





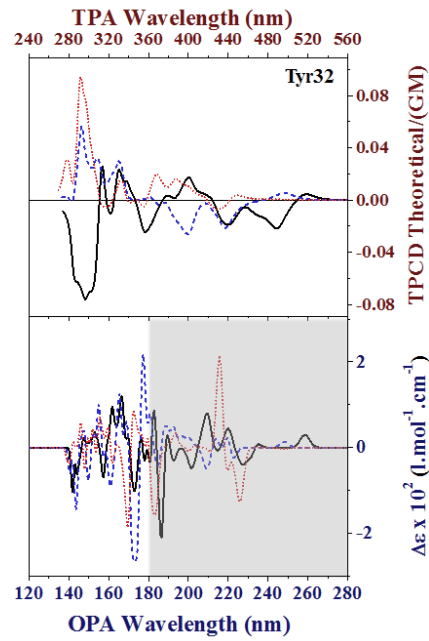
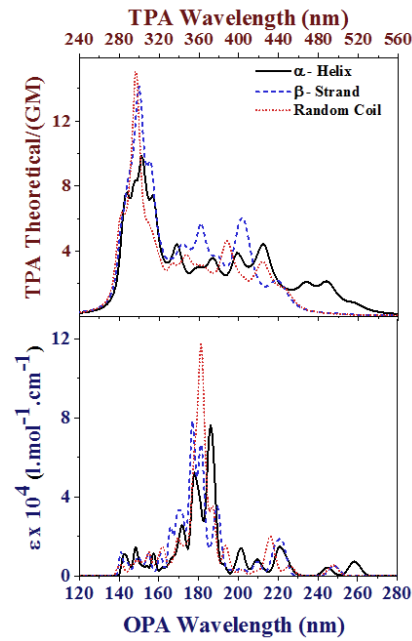
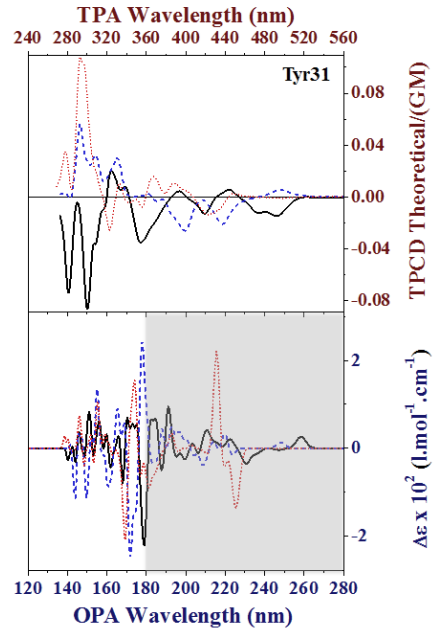
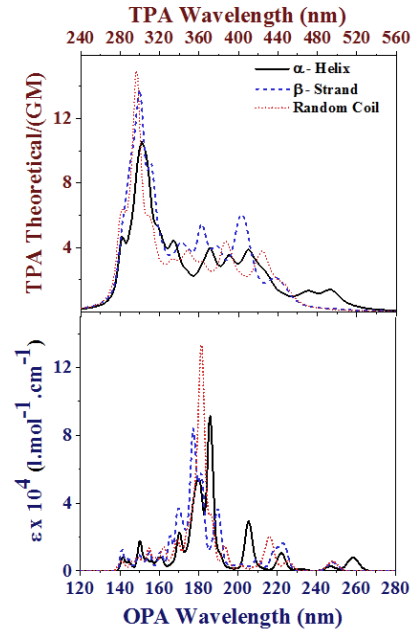
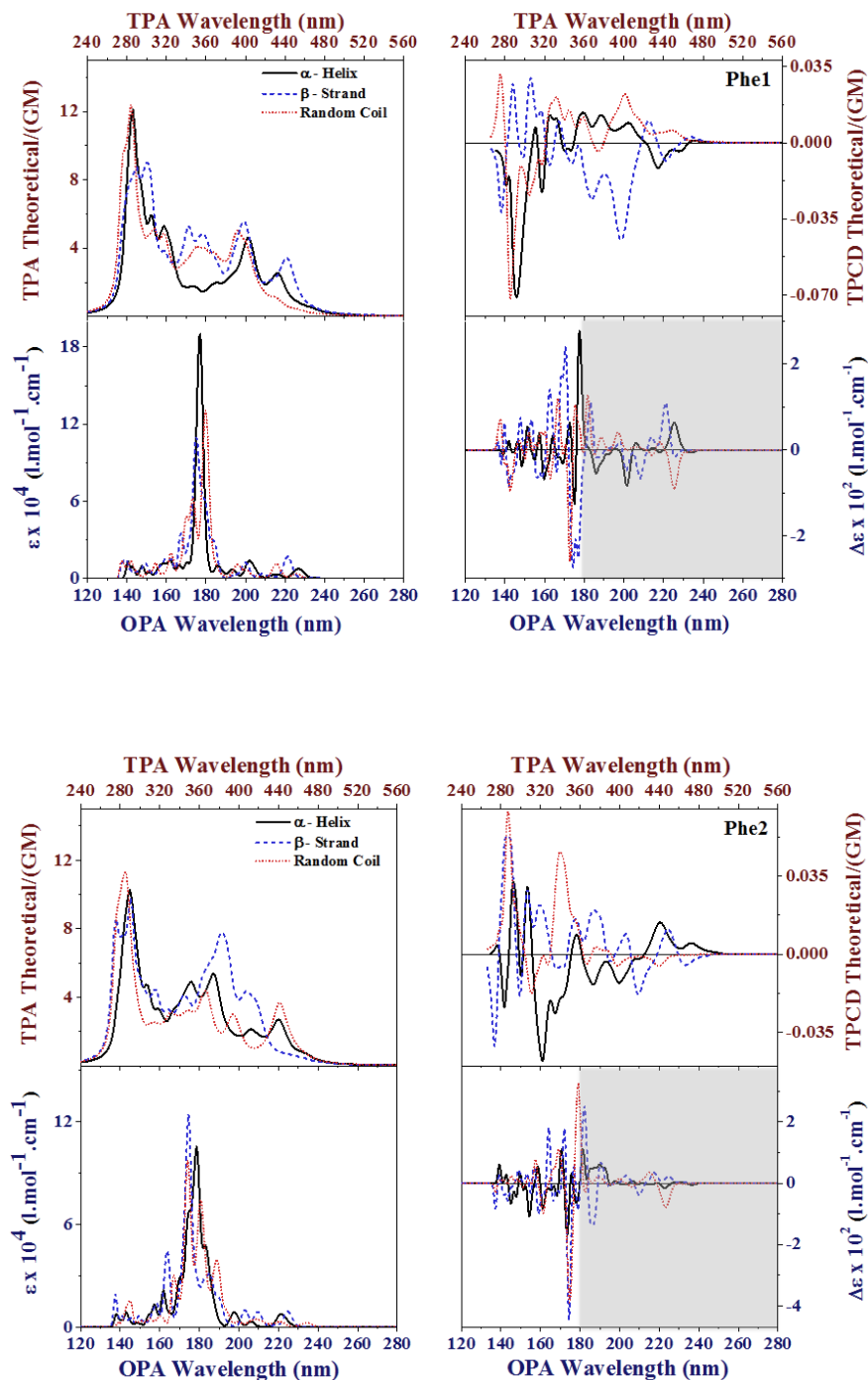


Figure S10. Comparative plots of TPA (top left), TPCD (top right), OPA (bottom left), and ECD (bottom right) spectra of all three Phe residues in their corresponding random-coil (red dotted line), α -helix (black solid line) and β -strand (blue dashed line) conformations. TD-DFT/B3LYP/6-311G(d)/80 excited states. Shaded area indicates where ECD is truly functional.



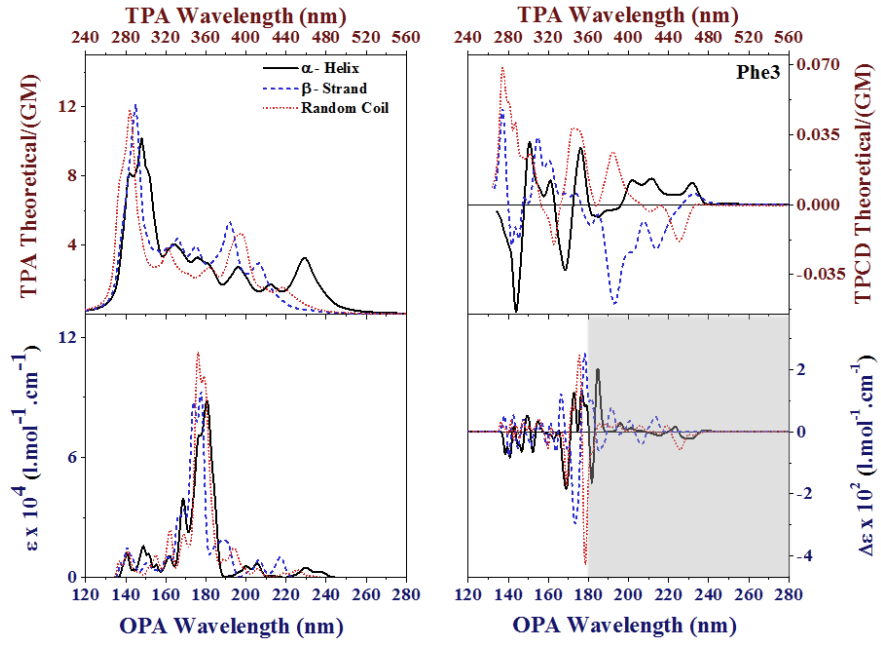


Figure S11. Stereochemical structures of L-histidine (left), L-tyrosine (right), and L-phenylalanine (down) models in β -strand conformation

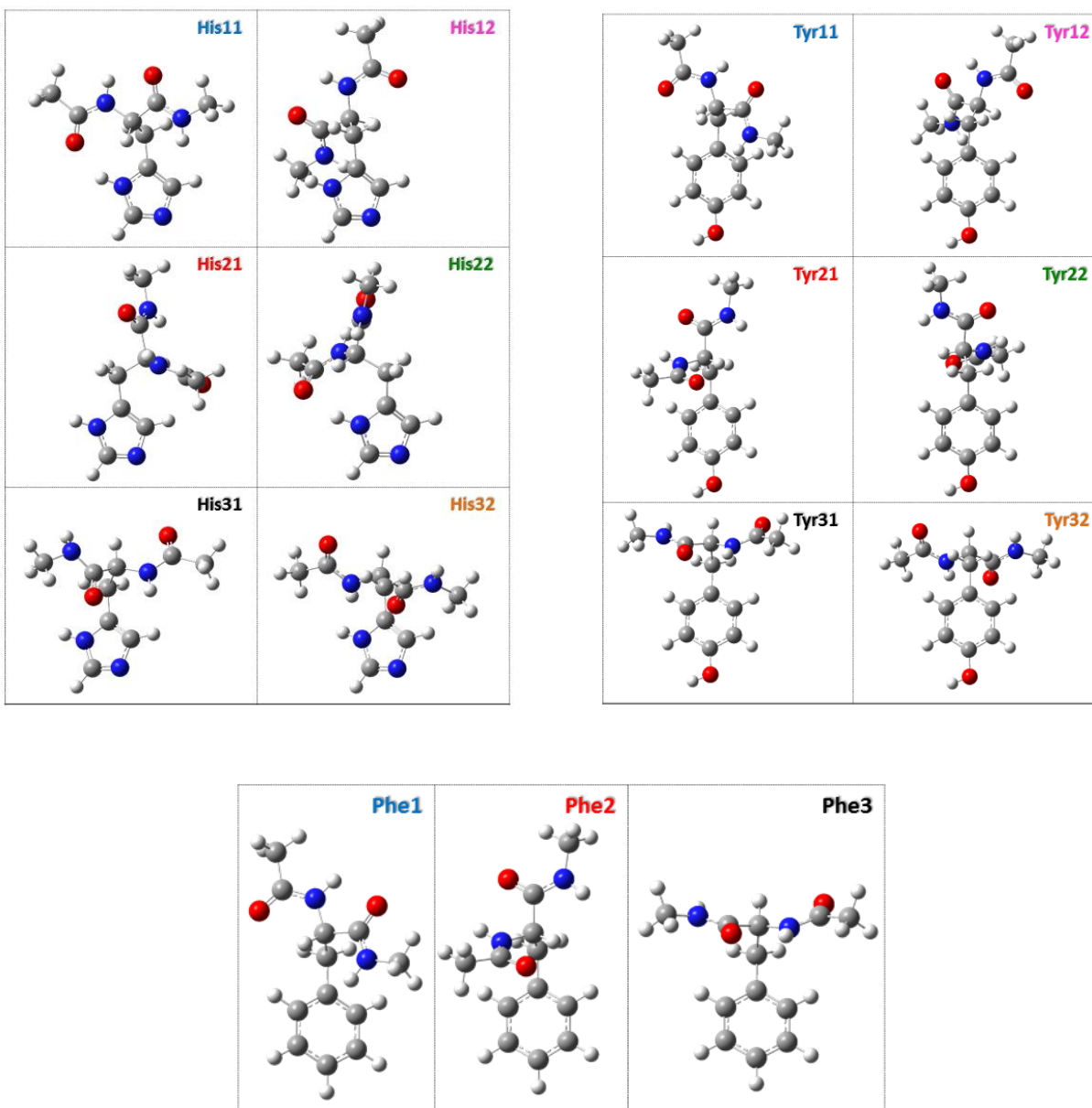


Figure S12. Stereochemical structures of L-histidine (left), L-tyrosine (right), and L-phenylalanine (down) models in α -helix conformation

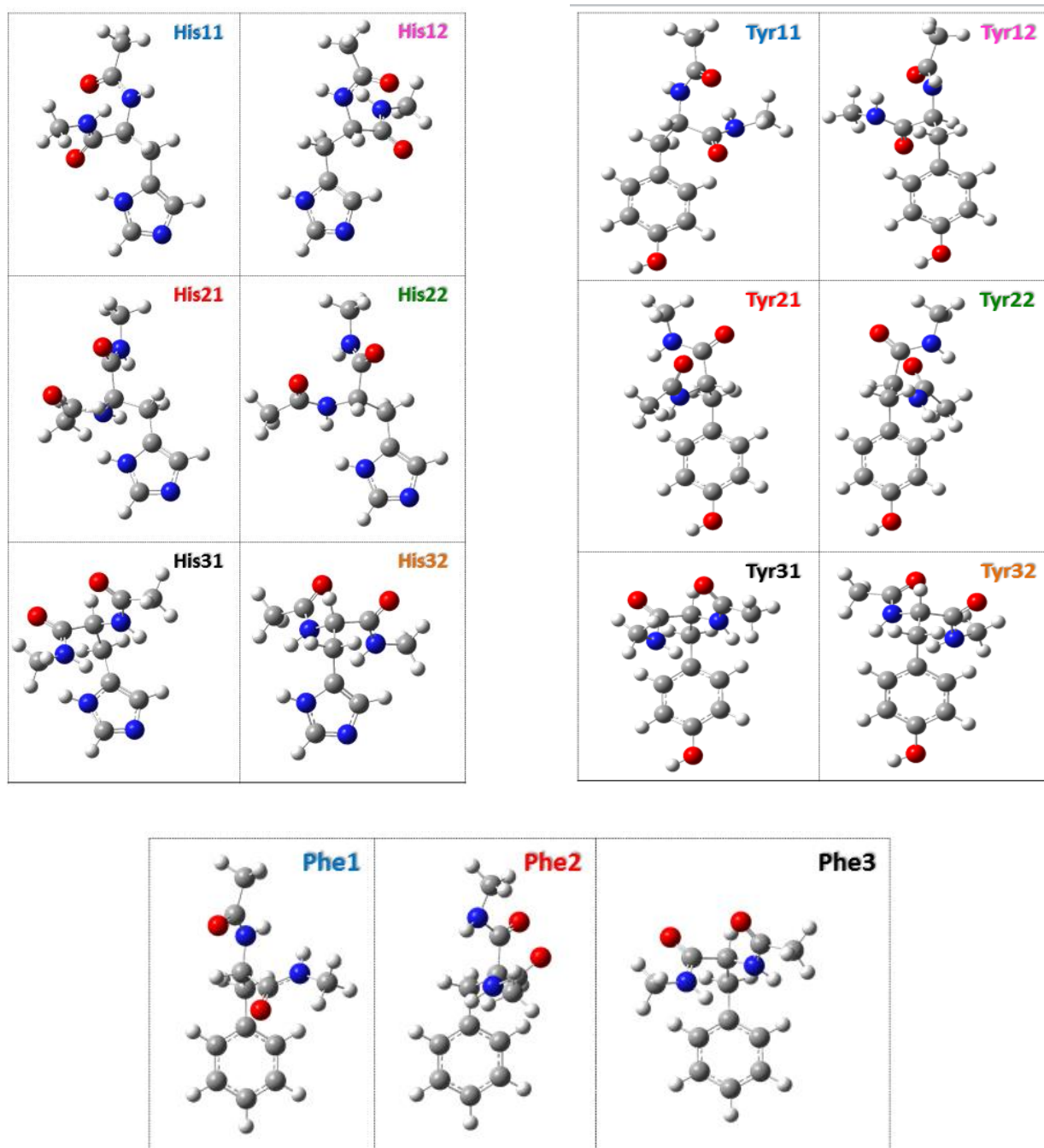


Figure S13. Comparative plots of TPA (left), TPCD (right) spectra of Tyr11 (red dotted line), His11 (black solid line) and Phe1 (blue dashed line) and TPA (left), TPCD (right) spectra of Tyr21 (red dotted line), His21 (black solid line) and Phe2 (blue dashed line) in random coil conformation. TPA and TPCD response for the lowest 80 electronic excited states of all optimized structures were computed with TD-DFT/ B3LYP/6-311G(d) in gas phase using Dalton 2011.

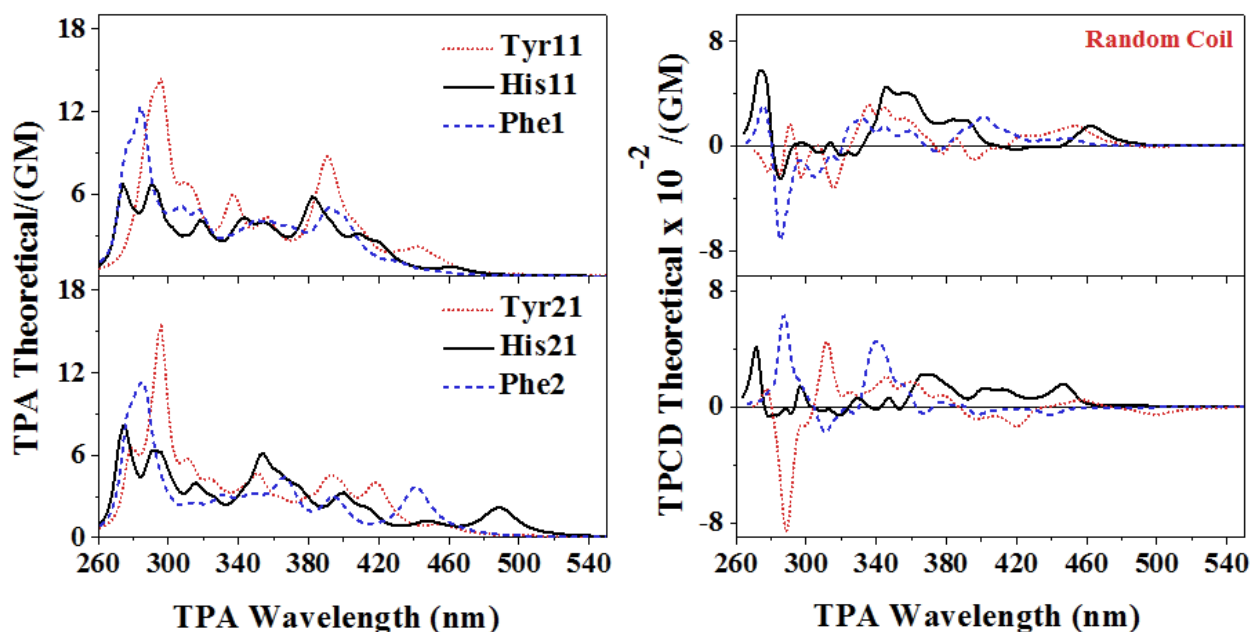


Figure S14. Comparative plots of TPA (left), TPCD (right) spectra of Tyr11 (red dotted line), His11 (black solid line) and Phe1 (blue dashed line) and TPA (left), TPCD (right) spectra of Tyr21 (red dotted line), His21 (black solid line) and Phe2 (blue dashed line) in β -strand conformation. TPA and TPCD response for the lowest 80 electronic excited states of all optimized structures were computed with TD-DFT/B3LYP/6-311G(d) in gas phase using Dalton 2011.

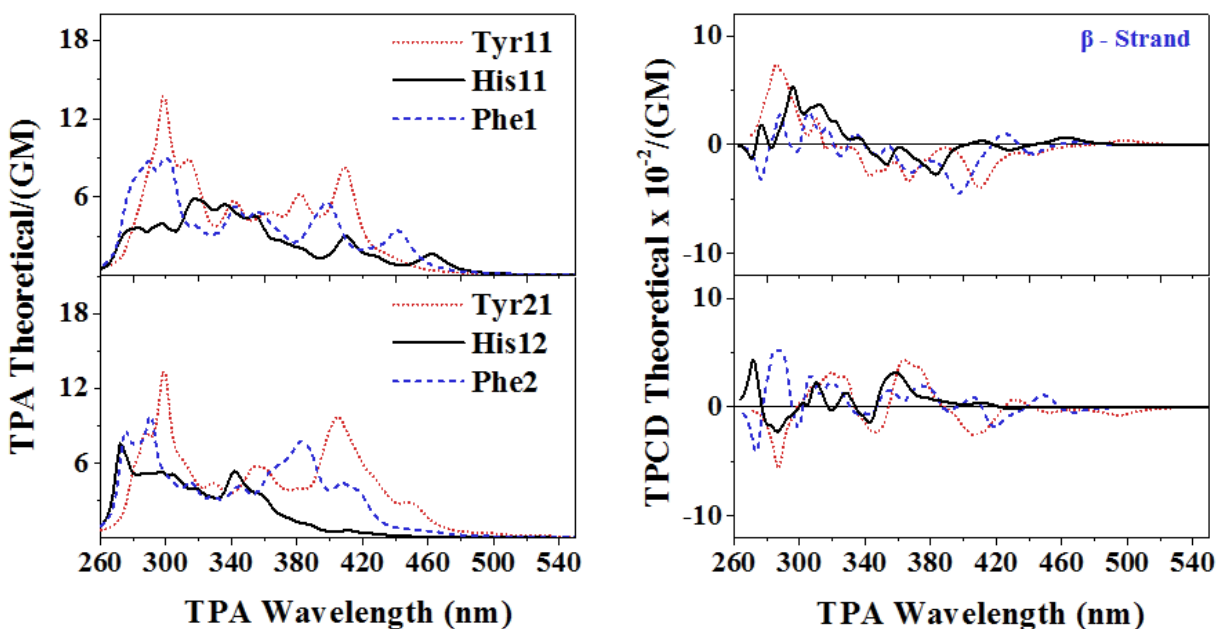
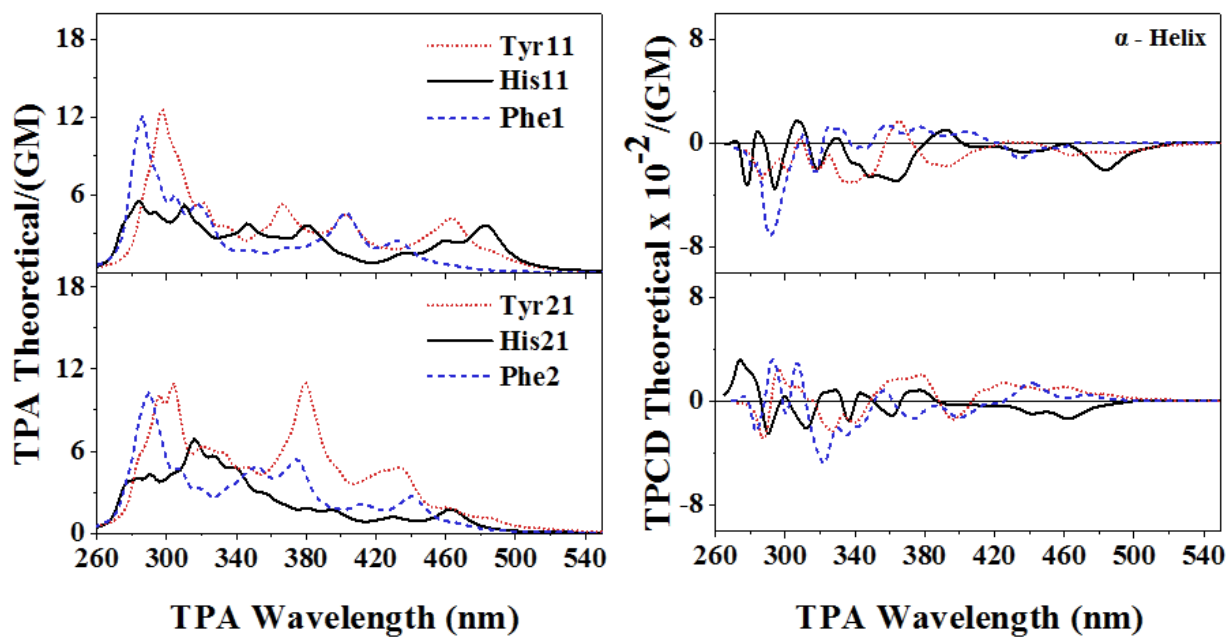


Figure S15. Comparative plots of TPA (left), TPCD (right) spectra of Tyr11 (red dotted line), His11 (black solid line) and Phe1 (blue dashed line) and TPA (left), TPCD (right) spectra of Tyr21 (red dotted line), His21 (black solid line) and Phe2 (blue dashed line) in α -helix conformation. TPA and TPCD response for the lowest 80 electronic excited states of all optimized structures were computed with TD-DFT/B3LYP/6-311G(d) in gas phase using Dalton 2011.



-
1. Dierksen, M.; Grimme, S., A Theoretical Study of the Chiroptical Properties of Molecules with Isotopically Engendered Chirality. *J. Chem. Phys.* **2006**, *124*, 174301.
 2. Runge, E.; Gross, E. K. U., Density-Functional Theory for Time-Dependent Systems. *Phys. Rev. Lett.* **1984**, *52*, 997-1000.
 3. Becke, A. D., Density-Functional Exchange-Energy Approximation with Correct Asymptotic Behavior. *Phys. Rev. A* **1988**, *38*, 3098-3100.
 4. Becke, A. D., Density-Functional Thermochemistry. III. The Role of Exact Exchange. *J. Chem. Phys.* **1993**, *98*, 5648-5652.
 5. Lee, C.; Yang, W.; Parr, R. G., Development of the Colle-Salvetti Correlation-Energy Formula into a Functional of the Electron Density. *Phys. Rev. B: Condens. Matter* **1988**, *37*, 785-789.
 6. Krishnan, R.; Binkley, J. S.; Seeger, R.; Pople, J. A., Self-consistent molecular orbital methods. XX. A basis set for correlated wave functions. *J. Chem. Phys.* **1980**, *72* (1), 650-654.
 7. McLean, A. D.; Chandler, G. S., Contracted Gaussian basis sets for molecular calculations. I. Second row atoms, Z=11-18. *J. Chem. Phys.* **1980**, *72* (10), 5639-5648.
 8. Frisch, M. J.; Trucks, G. W.; Schlegel, H. B.; Scuseria, G. E.; Robb, M. A.; Cheeseman, J. R.; Scalmani, G.; Barone, V.; Mennucci, B.; Petersson, G. A., *et al.* *Gaussian 09, Revision A.1*, Gaussian, Inc.: Wallingford CT, 2009.
 9. *Optical Spectra and Chemical Bonding in Transition Metal Complexes*. Springer: New York, 2004; Vol. 107.
 10. *Circular Dichroism: Principles and Applications*. 2nd ed.; VCH: New York, 2000.
 1. Dierksen, M.; Grimme, S., A Theoretical Study of the Chiroptical Properties of Molecules with Isotopically Engendered Chirality. *J. Chem. Phys.* **2006**, *124*, 174301.

2. Runge, E.; Gross, E. K. U., Density-Functional Theory for Time-Dependent Systems. *Phys. Rev. Lett.* **1984**, *52*, 997-1000.
3. Becke, A. D., Density-Functional Exchange-Energy Approximation with Correct Asymptotic Behavior. *Phys. Rev. A* **1988**, *38*, 3098-3100.
4. Becke, A. D., Density-Functional Thermochemistry. III. The Role of Exact Exchange. *J. Chem. Phys.* **1993**, *98*, 5648-5652.
5. Lee, C.; Yang, W.; Parr, R. G., Development of the Colle-Salvetti Correlation-Energy Formula into a Functional of the Electron Density. *Phys. Rev. B: Condens. Matter* **1988**, *37*, 785-789.
6. Krishnan, R.; Binkley, J. S.; Seeger, R.; Pople, J. A., Self-consistent molecular orbital methods. XX. A basis set for correlated wave functions. *J. Chem. Phys.* **1980**, *72* (1), 650-654.
7. McLean, A. D.; Chandler, G. S., Contracted Gaussian basis sets for molecular calculations. I. Second row atoms, Z=11–18. *J. Chem. Phys.* **1980**, *72* (10), 5639-5648.
8. Frisch, M. J.; Trucks, G. W.; Schlegel, H. B.; Scuseria, G. E.; Robb, M. A.; Cheeseman, J. R.; Scalmani, G.; Barone, V.; Mennucci, B.; Petersson, G. A., *et al.* *Gaussian 09, Revision A.1*, Gaussian, Inc.: Wallingford CT, 2009.
9. *Optical Spectra and Chemical Bonding in Transition Metal Complexes*. Springer: New York, 2004; Vol. 107.
10. *Circular Dichroism: Principles and Applications*. 2nd ed.; VCH: New York, 2000.
11. Meierhenrich, U. J.; Filippi, J.-J.; Meinert, C.; Bredehöft, J. H.; Takahashi, J.-i.; Nahon, L.; Jones, N. C.; Hoffmann, S. V., Circular Dichroism of Amino Acids in the Vacuum-Ultraviolet Region. *Angew. Chem. Int. Ed.* **2010**, *49* (42), 7799-7802.